J. Membrane Biol. 39, 133–157 (1978)

Nucleoside Transport in Mammalian Cell Membranes

III. Kinetic and Chemical Modification Studies of Cytosine-arabinoside and Uridine Transport in Hamster Cells in Culture

O. Heichal, O. Bibi, J. Katz, and Z.I. Cabantchik*

Biophysics Group, Institute of Life Sciences, Hebrew University, Jerusalem, Israel

Received 16 March 1977; revised 30 August 1977

Summary. Transport of the nucleoside analog cytosine-arabinoside (CAR) in transformed hamster cells in culture has been studied in conditions of minimal metabolic conversion. Uptake (zero-trans in) properties at 20 °C over a limited range of CAR concentrations were characterized by a K_m of 350 μM and a maximal velocity (V) of 780 μM · min^{-1} ($V/K_m = 2.28\ min^{-1}$). Equilibrium exchange at 20 °C over a wider range of concentrations was best described by a saturable component with a K_m of 500 μM and a v of 1230 μM · min^{-1} ($V/K_m = 2.26\ min^{-1}$) and either a saturable component of high K_m or a nonsaturable component of $k = 0.3\ min^{-1}$. For the saturable component, the v/K_m values were similar in both procedures.

CAR transport was inhibited by various metabolizable nucleosides. Uptake of some of these nucleosides was inhibited by CAR. CAR transport and uridine uptake were inhibited in a reversible but partially competitive fashion by high affinity probes like S-(*p*-nitrobenzyl-6-mercaptoinosine (NBMI) ($K_i < 0.5$ nM) and in an irreversible fashion by SH reagents such as N-ethylmaleiimide (NEM). The organomercurial *p*-hydroxymercuribenzene sulfonate (pMBS) markedly stimulated transport of these nucleosides, but also markedly potentiated the inhibitory effects of either NBMI or NEM. These effects are interpreted either in terms of models which invoke allosteric properties or in terms of two transport systems which display distinct chemical susceptibilities to externally added probes.

Recent studies with analogs of nucleic acid bases and nucleosides which display cytotoxic effects within mammalian cells have focused interest on the route and mechanisms of permeation of these compounds [10, 18, 19, 22]. That membrane transport may be an important determinant of cytotoxicity was suggested by the fact that tumor cell resistance to anticancer agents, many of which are analogs of naturally occurring substances, may be related to alteration in specific membrane

* *Present address and for reprint requests:* Laboratory of Kidney and Electrolyte Metabolism, NHLBI, National Institutes of Health, Building 10, Room 6N320, Bethesda, Maryland 20014.

0022-2631/78/0039-0133 $4.80

transport mechanisms [10]. Studies of uptake of nucleosides and other nutrients have also suggested a role of transport in the control of cell growth and neoplasia [5, 16, 24]. However, in uptake studies of metabolizable permeants, transport could not be easily separated from intracellular metabolism. For some nucleosides, an enzymatic reaction at the membrane level was invoked as an obligatory component of the transport process [14, 29]. Two different approaches were successfully utilized in an attempt to study transport separately from metabolism. One has employed vesicles derived from plasma membranes deprived of intracellular enzymes [15, 29]. The other has employed intact cells deficient in enzymes that process a particular nucleoside, or metabolically poisoned cells that retained their nucleoside transport activity [27, 28].

In the present work, cytosine-arabinoside (CAR)[1] was used as the permeant nucleoside to study the nucleoside transport system of hamster cells in culture and the mechanism of action of potent and specific inhibitors of nucleoside transport. Previous uptake studies have shown that CAR penetrates mammalian cells via facilitated mechanisms and quickly attains equilibrium with the surroundings [18, 19, 22]. Various mammalian cells can either deaminate or phosphorylate CAR [11, 18, 32, 33]. However, in hamster cells, these processes were shown to be considerably slower than transport and could be minimized, in some instances, to levels where intracellular metabolic conversions did not interfere with transport measurements.

The inhibitor used in this study, S-nitrobenzyl-6-mercaptoinosine (NBMI), has been shown to specifically block nucleoside transport in red blood cells [2, 3, 23, 25] and nucleoside uptake in a variety of mammalian cells in culture [8, 9] at concentrations below 1 nM. We have previously shown, in cultured cells, that the specific inhibitory effect of NBMI on uridine and other nucleoside uptake systems could be tentatively explained in terms of an allosteric modulatory mechanism [8, 9, 20]. However, since the inhibition studies were conducted with metabolizable permeants, it remained to be proven that metabolic conversion was not rate limiting either in the absence or in the presence of NBMI so that the inhibitory effects could be related to transport of nucleosides. Evidence supporting our previous view (9) and new aspects of chemical

1 *Abbreviations:* CAR, cytosine arabinoside; NEM, N-ethylmaleimide; PBS, phosphate buffered saline; MCT, 20-methylcholanthrene transformed; NBMI, S-nitrobenzyl-6-mercaptoinosine; NBB, *p*-nitrobenzylbromide; *p*MBS: *p*-hydroxymercuribenzene sulfonate; *p*MB-dextran: *p*-hydroxymercuribenzo-amidoethyl-dextran (mol wt 10,000).

modification of nucleoside transport systems constitute the main line of this work.

Materials and Methods

Radiochemicals were obtained from the following sources: (^{3}H) uridine (10 Ci/mmole) and (^{3}H) thymidine (8 Ci/mmole) from Radioisotope Unit, NRC-Negev, Israel AEC, Beer Sheva, and (^{3}H) cytosine-arabinoside (14 Ci/mmole) from the Radiochemical Center (Amersham, U.K.). Chemicals were obtained from the following sources: nucleosides and mercaptonucleosides from Sigma Chemical Co., *p*-hydroxymercuribenzene-sulfonic acid Na salt (*p*MBS) and N-ethylmaleimide (NEM) from K and K Laboratories and *p*-nitrobenzylbromide (NBB) from Fluka (Switzerland). S-(*p*-nitrobenzyl)-6-mercapto-9-β-D-ribofuranosyl purine (NBMI) was synthesized from NBB and 6-mercapto-inosine in N,N′-dimethylformamide/K_2CO_3 and was purified and crystallized as previously described [21, 25].

MCT is a cell line derived from a tumor in golden hamsters after inoculation of 10^6 Ham cells (20-methylcholanthrene transformed hamster embryo cells) [17]. The cells were grown in Dulbecco's modified Eagle's medium (DMEM) supplemented with 3 % fetal calf serum (Gibco), 10 % Triptose phosphate, 2 mM glutamine and antibiotics (streptomycin, 400 µg/ml; penicillin, 400 U/ml; neomycin, 4 µg/ml and kanamycin, 3 µg/ml). Cells were counted after detachment from dishes by trypsinization.

Transport Studies

Cells were plated on 5 cm plastic culture dishes (Nunc, Denmark) at $0.5–1.0 \times 10^6$ cells/dish and grown to different densities ($0.5–8 \times 10^6$ cells) in a humidified CO_2 (5 %) incubator at 37 °C. For transport measurements, cells were washed thrice with 5-ml aliquots of phosphate-buffered saline (PBS, pH 7.4) and preincubated with 2 ml of the same buffer for 10 min at room temperature (22–24 °C). At this point, some dishes were taken for cell counting. For rapid uptake studies (10 ± 2 sec sampling times), the extracellular PBS was aspirated, the cells were placed on a thermostated plate at 20 ± 1 °C, and 1 ml of a radioactive nucleoside (20 °C) was added (1 µCi/ml, unless specified otherwise). At defined periods of time dishes were quickly transferred to a metal plate immersed in an ice bath (0 °C), and the extracellular solution was quickly aspirated (1–2 sec, *see* Fig. 1). The dishes were immediately flushed, either continuously with 25 ml of PBS at 0 °C or repetitively with 5-ml portions of PBS at 0 °C while the extracellular solutions were continuously being aspirated. The procedure of washing the cells was gentle, efficient, and quick inasmuch as: (i) the cells were not dislodged from the dishes, (ii) the volume of washing solution was adequate for removing extracellular labelled material, leaving the label sequestered within the cells virtually unaffected (Fig. 2), and (iii) the time lag before dispensing the stopping fluid (PBS, 0 °C) was approximately 2 sec. With practice, a full cycle of stopping fluxes and washing the extracellular medium was completed in less than 15 sec. The times at which the stopping fluid was added were used for computation of flux rates. The intracellular label was quantitatively extracted with 1 ml TCA (10 %) for 15 min at 0 °C, and 0.5 ml was taken for counting of radioactivity using a Triton-toluene based liquid and a Tricarb Liquid Scintillation Spectrometer. Samples were in duplicate and occasionally in tri- and quadruplicate. Protein determinations (Lowry) were preformed on the TCA residue after solubilization with 1 N NaOH. With (^{3}H) CAR as the test nucleoside, the radioactivity associated with the TCA insoluble residue was less than 3 % of the value found in the TCA extract.

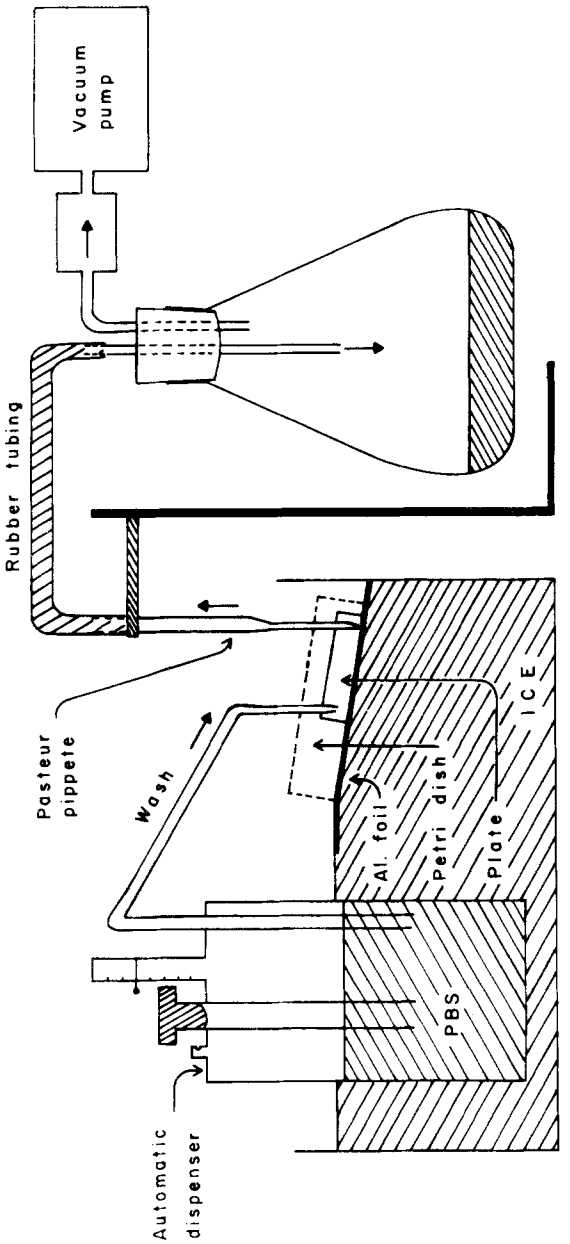

Fig. 1. Set up for washing cells adhered to plastic dishes. Plastic dish (*plate*) is placed on a Petri dish of approximately 10 cm diameter on a slant aluminum foil surface of an ice bath. The tip of a Pasteur pipette is placed on the lower side of the plastic dish and the solution is aspirated into a collecting flask. An extension of an automatic pipettor is placed on the upper side of the dish. The pipettor can be actuated remotely with a foot-extension, or an electrical drive

Transport of (^{3}H) CAR was also measured under equilibrium exchange conditions (efflux). Cells were preincubated at 22 °C with (^{3}H) CAR at different concentrations until equilibrium was reached (normally not more than 10 min, even for the highest concentration of substrate used, 10 mM). The extracellular medium was then aspirated. At time zero, either 5 ml of ice cold PBS were added (zero time sample) or 5 ml of the respective unlabelled solutions of CAR (20 °C) were added, and the intracellular label

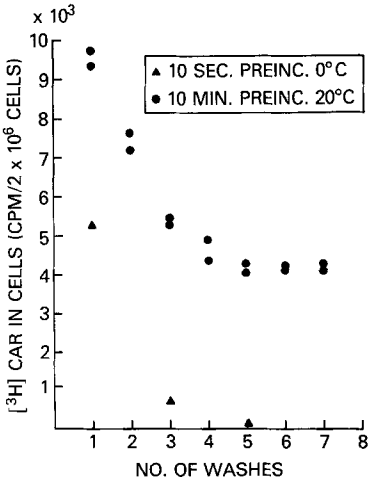

Fig. 2. Effect of washing on (^{3}H) CAR in cells. Cells (2×10^6/dish) were loaded with 50 μM (^{3}H) CAR (1×10^6 cpm/ml) either for 10 sec at 0 °C or for 10 min at 20 °C, placed on ice, and washed with 5-ml aliquots of ice cold PBS. Each point represents (^{3}H) label of an individual dish after a specified number of washes. The density of cells (number of cells per dish) was constant within each of the two experiments

was measured as described for the uptake studies. Duplicate plates were also left for 10–20 min at room temperature in order to obtain the amount of labelled material left in the cells at equilibrium with the exchange solution (cpm ∞). The relative amounts of (^{3}H) CAR remaining in the cells at different times, t, are given as [cpm (t) − cpm (∞)]/[cpm (0) − cpm (∞)] = (exp) − kt. The rate constant, k, was obtained by linear regression (correlation coefficients were normally between 0.985 − 0.995). The transport rates were calculated as $v = k[S]$.

For zero-trans influx (net uptake), cells were exposed to various concentrations of (^{3}H) CAR for various periods of time (t) at 20 °C. Duplicate samples were also exposed for 5-10 min at 20 °C until the label reached equilibration [cpm (∞)]. Zero time values were obtained by exposing precooled cells to solutions containing (^{3}H) CAR at 0 °C for 10 sec. Initial rates of efflux were obtained from the linear part of the uptake profiles and were calculated as $v = [S] \cdot (t)^{-1} \cdot$ [cpm (t) − cpm (0)]/[cpm (∞) − cpm (0)]. Uridine and thymidine uptake were performed in a similar fashion or as previously described [9].

Calculations of kinetic parameters were obtained by best fits using nonlinear regression programs to analyze data according to (i) a single Michaelis-Menten kinetic component $v = V \cdot [S]/(Km + [S])$, (ii) two Michaelis-Menten components $v = (V^I \cdot [S])/(Km^I + [S]) + (V^{II} \cdot [S])/(Km^{II} + [S])$, or (iii) a single Michaelis-Menten component and a nonsaturable component $v = (V \cdot [S]/(Km + [S])) + k[S]$. The method is based on the Levenberg-Marquand technique and the computations were made at the facilities of the Hebrew University Computer Center. Alternatively, the kinetic parameters were obtained from best fits using a linear regression program to analyze the linearized form of the Michaelis-Menten expression $(v/[S]) = (K_m/V) + ([S]/V)$. These calculations were performed on a Wang 2200 computer.

For metabolic conversion studies, cells preincubated with (^{3}H) CAR for up to 10 min at 20 °C were washed with ice-cold PBS, and the radioactivity was extracted with either

3% TCA or with 0.4 M perchloric acid (PCA). After either neutralization of the PCA with KOH, cooling to 0 °C for 30 min and centrifugation or removal of TCA by ether extraction, the cell extract was analyzed by thin layer chromatography on either cellulose or silica gel-coated aluminum plates (Merck) using either 0.1 M potassium phosphate buffer, pH 5.8, ammonium acetate, 1 M, pH 5.0/ethanol, 95% (3:7, v/v) or *n*-butanol/water/formic acid (77:13:10, v/v/v) [14]. Plates were cut into 0.7 to 0.5-cm strips, placed in scintillation vials with 0.1 ml water, and counted for (^{3}H) with a triton-toluene based scintillation fluid.

Results

Time Course of Nucleoside Uptake in MCT Hamster Cells

The uptake of uridine (U), thymidine (T) and of cytosine-arabinoside (CAR) were carried out at concentrations approximately 1/5 of the K_m value of uptake of the individual nucleoside (Fig. 3). In the early phases of uptake (i.e., up to 60 sec), the amount of U and T taken up by the cells increased in a linear fashion. However, in this phase, the uptake of CAR was linear only up to 30 sec and reached a plateau value which was presumably the equilibrium value of (^{3}H) CAR with respect to the external solution, inasmuch as the plateau value attained by CAR at

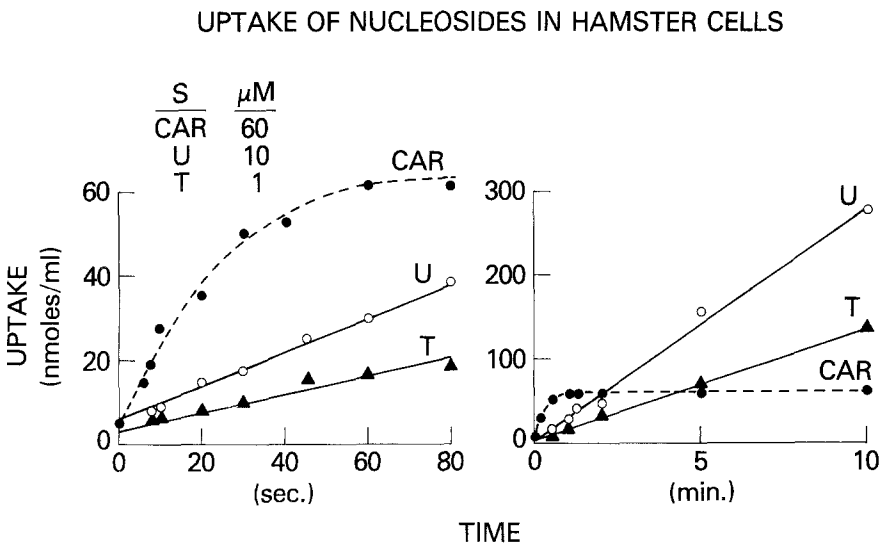

Fig. 3. Early phases of nucleoside uptake in MCT hamster cells in culture. Nucleoside uptake (1×10^6 cpm/ml) was measured in 2×10^6 cells per dish or 4 μl equivalent cell volume. The external concentrations of (^{3}H) nucleoside (*S*) were: U (uridine) 10 μM, *T* (thymidine) 1 μM, and CAR (cytosine-arabinoside) 60 μM. The zero time values for the three nucleosides were essentially the same (±10%) in these experiments

20 °C was invariant with time for up to 10 min. The uptake of the metabolizable nucleosides U and T, however, increased in a linear fashion. After 10 min incubation, the cellular concentrations attained were 25 and 130-fold higher than those of the respective external solutions.

At zero-time uptake (10–20 sec exposure at 0 °C) there was always a small but discrete amount of either extracellular binding or uptake component which ranged from 2 to 10% of labelled nucleoside concentration in the external solution. These values were taken into account and subtracted accordingly. In uptake studies with CAR in the range 20–2,000 μM at constant (^{3}H) radioactivity, the value of radioactivity found in the cells at 5 min was essentially the same for all CAR concentrations and was constant for at least 5 more min at 20 °C. Since similar results were obtained with 3-0-methyl glucose, a nonmetabolizable sugar, it was assumed that the (^{3}H) reaches equilibrium with the external solutions and that the radioactivity inside the cell represented primarily the internal volume of cells (i.e., cellular nucleoside free volume). The (^{3}H) labelled material extracted from cells after 8 min incubation was indistinguishable from (^{3}H) CAR as analyzed by thin layer radiochromatography (*see* Methods). Therefore, in 5–10 min of incubation at 20 °C, the metabolic conversion of CAR by MCT cells was negligible, and transport was the rate-limiting step of CAR uptake.

Internal Volume of Cells

Plates with different numbers of cells were used for the determination of the nucleoside volume (i.e., internal cell volume) and for cell protein (Fig. 4). At densities of up to 6×10^6 cells per plate, the protein content of the cells and the internal cellular volume were linear with the number of cells. The protein content amounts to about 10% of the total cell weight (assuming cells have a density of 1 g/ml). In PBS medium the volume occupied by 10^6 MCT hamster cells is 2 μl and their protein content 0.2 mg. These values were also confirmed using 3-0-methyl-glucose as the nonmetabolizable substrate. They were independent of the specific activity of the labeled species. The equilibrium levels of (^{3}H) CAR and the above coefficients were used to determine the actual concentration of compounds that penetrated into the cells. This method was found more reliable, reproducible, and convenient than counting the number of cells per plate.

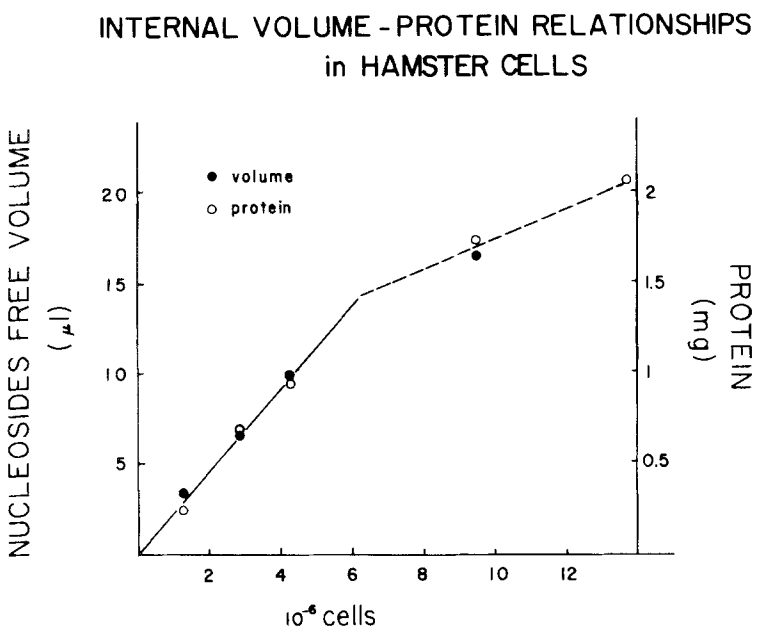

Fig. 4. Relationship between number of cells, cell protein, and cell internal volume (calibration curve). Cells at different densities were measured for protein (triplicates) and for equilibrating levels of (^{3}H) cytosine-arabinoside (quadriplicates). The SEM of each experiment was smaller than the size of the circle in the figure

Kinetic Properties of CAR Transport

Transport of CAR was measured by the zero-trans influx procedure (i.e., uptake) and by the exchange efflux procedure [2, 36]. The Michaelis-Menten and reciprocal plots of CAR uptake are shown in Fig. 5 and of CAR exchange in Fig. 6 (*B* and *C*). Initial transport rates v were obtained from 10–20 sec uptake measurements, while uptake was demonstrably linear with time. However, above 1 mM (^{3}H) CAR, the present technique did not allow estimation of initial uptake rates. The rates of exchange, v, were computed from $v = k \cdot [S]$ in which $[S]$ was CAR concentration. The rate constant k was obtained from the integrated rate equation given in *Materials and Methods*. The kinetic constants related to uptake and exchange were obtained by either linear or nonlinear regression analysis (Table 1).

For uptake, the two analytical procedures gave similar kinetic constants (V, K_m) and similar V/K_m ratios. For up to 1 mM substrate, the data could well be fitted to a single Michaelis-Menten component.

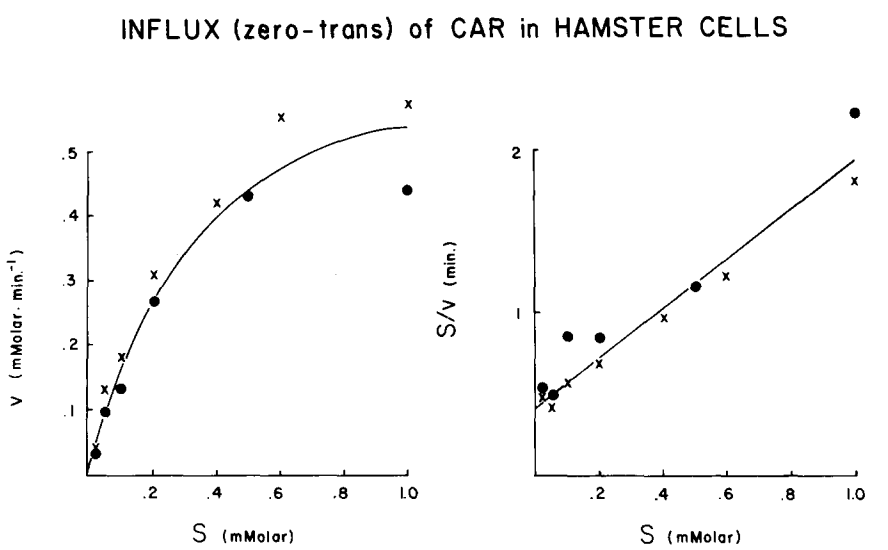

Fig. 5. Kinetics of CAR influx (zero-trans). Cells (5 µl equivalent volume) were incubated with various concentrations of (^{3}H) CAR (S) and the initial rates of uptake, v, were calculated. Data of two separate experiments (crosses and circles, each performed in duplicates and averaged) are presented as Michaelis-Menten (left) (v against S) and reciprocal plots (right) (S/v against S). The left graph shows a nonlinear regression line drawn by the computer for a single Michaelis-Menten component: $V=795\pm105$ µM min^{-1} and $K_m=350\pm110$ µM. ($V/K_m=2.26$ min^{-1}.) The right graph shows the linear regression line for $V=690\pm70$ µM min^{-1} and $K_m=295\pm45$. ($V/K_m=2.34$.)

Incorporation of additional saturable or nonsaturable components did not improve the data or the related correlation coefficients (Table 1).

For the exchange procedure, the kinetic constants obtained from either linear or nonlinear regression analysis of single Michaelis-Menten components were substantially higher than the corresponding kinetic constants of uptake. V/K_m values, however, were substantially lower than those of uptake. Only when an additional exchange component was included in the analysis, could the kinetic constants be made more comparable to the respective constants of uptake. This also resulted in a new V/K_m value, which became virtually the same as that of uptake, validating the assumption of the second component. The presence of this additional component of exchange became apparent at high concentrations of substrate ($S>5$ mM). However, data obtained with up to 20 mM substrate were not sufficient to ascertain whether that component was also of a saturable nature. If in fact it was, then its K_m value had to be considerably higher than that associated with uptake (i.e., at least 50

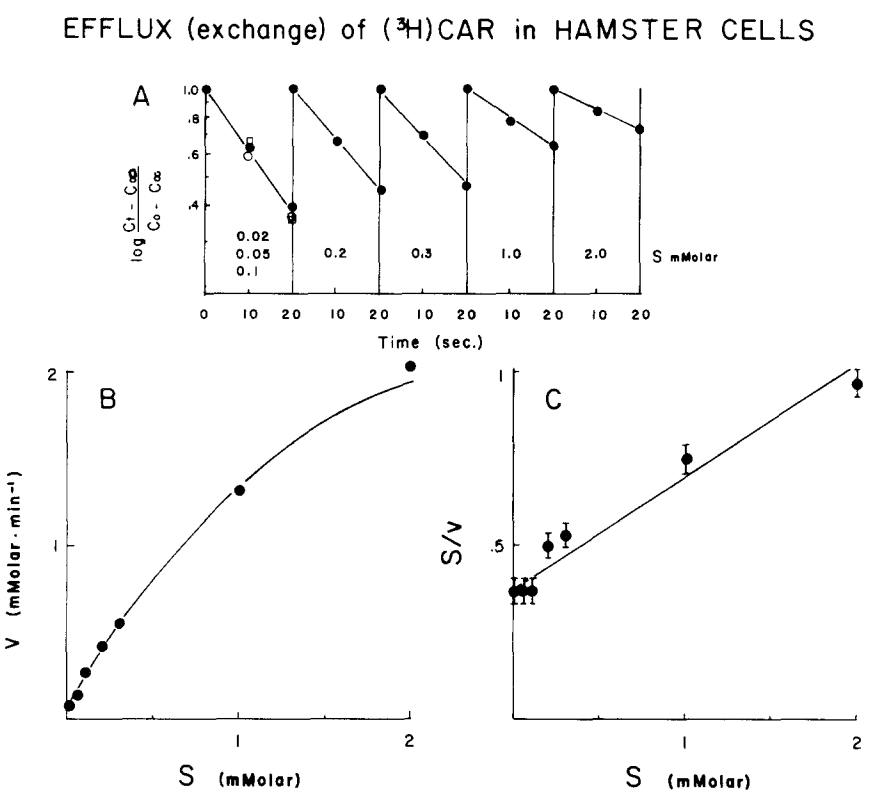

Fig. 6. Kinetics of CAR efflux (equilibrium exchange). Cells (6.2 µl equivalent volume) were equilibrated with various concentrations of (^{3}H) CAR (constant counts 1×10^6 cpm/ml). The extracellular loading solution was removed, and efflux was initiated with 5 ml of the respective CAR solutions. (*A*): Fractional radioactivity remaining in cells plotted against time; rate constants, k, are computed by linear regression. (*B*): Michaelis-Menten plots. Efflux parameters were calculated from data shown in *A*: $v = k[S]$. (*C*): Reciprocal plots of single Michaelis-Menten component using data shown in *B*. Kinetic constants obtained from linear regression analysis were: $v = 3850 \pm 380$ µM · min^{-1} and $K_m = 2320 \pm 475$ µM. ($V/K_m = 1.66$. *See also* Table 1.)

times higher). The computer simulated curves for a single component and for multiple components are displayed in Fig. 7.

In order to test the specificity properties of the CAR transport system of MCT cells, the effects of various nucleosides on (^{3}H) CAR uptake were studied (Fig. 8). The latter were measured after simultaneous addition of substrate and inhibitor. Uptake was followed from 10 to 60 sec, depending on the concentrations of inhibitor. Uptake of CAR was measured at a constant concentration of substrates S ($S \ll K_m$) and increasing concentrations of inhibitor (I). Data is given as 1/fractional

Table 1. Kinetic constants of (^{3}H) CAR transport in hamster cells in culture[a]

Method[b]	Zero-trans in				Exchange out			
	V	K_m	V/K_m	k	V	K_m	V/K_m	k
I	590 ± 70	295 ± 45	2.34	–	3070 ± 380	1850 ± 475	1.66	–
II	791 ± 110	350 ± 110	2.26	–	3660 ± 405	2120 ± 450	1.72	–
III	783 ± 125	343 ± 135	2.28	$<10^{-6}$	1230 ± 340	503 ± 146	2.26	0.3 ± 0.1

[a] V and K_m are given in μM min^{-1} and μM, respectively. V/K_m and k are given in min^{-1}.
[b] Transport parameters were calculated from original data shown in Figs. 5 and 6. Method *I* is a linear regression analysis of the S/v *vs.* S linearized Michaelis-Menten formula. Method *II* is a nonlinear regression analysis of the v *vs.* S Michaelis-Menten formula. Method *III* is the same as *II* but with an additional component $k.S$ incorporated in the Michaelis-Menten formula (*see* Methods). Simulated curves based on the kinetic parameters of exchange (Method *III*) are shown in Fig. 7.

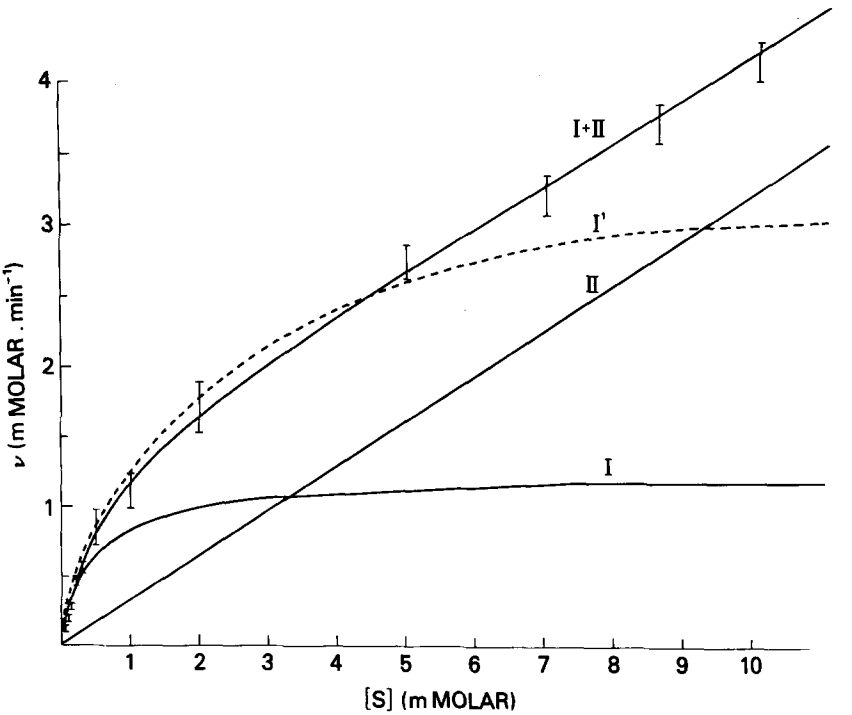

Fig. 7. Kinetic components of CAR exchange. Experimental points taken from Fig. 6 and from additional experiments are averaged and range of values (±SEM) are presented within bars. Data are analyzed by nonlinear regression method in terms of $v^{I+II}=v^I+v^{II}$ where $v^I=V^I[S]/(K_m^I+[S])$ and $v^{II}=k^{II}[S]$. *I*, *II*, and *III* are theoretical curves (solid lines) generated by computer using the kinetic parameters derived from nonlinear regression analysis of two component kinetics (Table 1). Curve *I'* (broken line) is the theoretical curve for a single Michaelis-Menten component using the kinetic parameters derived from nonlinear regression analysis (Table 1)

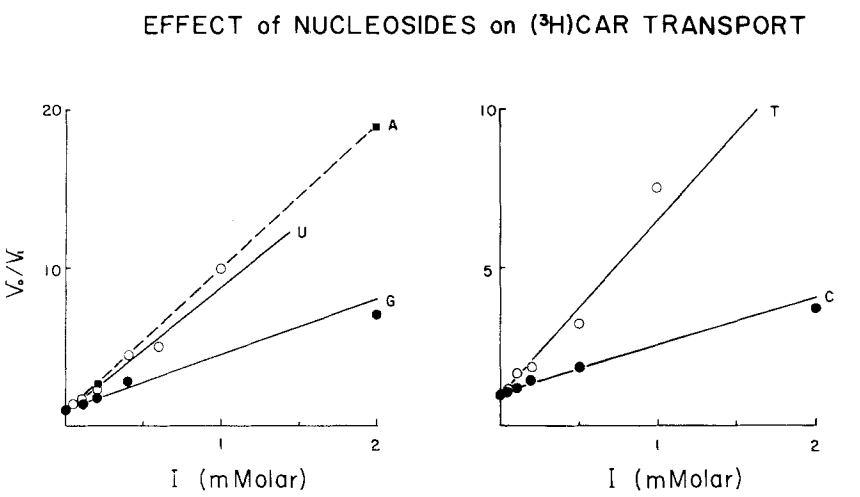

Fig. 8. Effect of various nucleosides on (^{3}H) CAR transport. Uptake of (^{3}H) CAR (50 μM, 1×10^6 cpm/ml) measured in the absence (V_0) or presence (V_I) of increasing concentrations of nucleosides (I) and plotted as V_0/V_I *vs.* (I) · ($V_0/V_I = 1$/fractional transport). The nucleoside concentration that reduced V_0 by 1/2 (ID_{50}) was obtained from the linear regression line. The ID_{50} values (in μM) were: for adenosine (A), 60±15; for uridine (U), 100±36; for guanosine (G), 390±90; for thymidine (T), 180±35; and for cytidine (C), 880±130

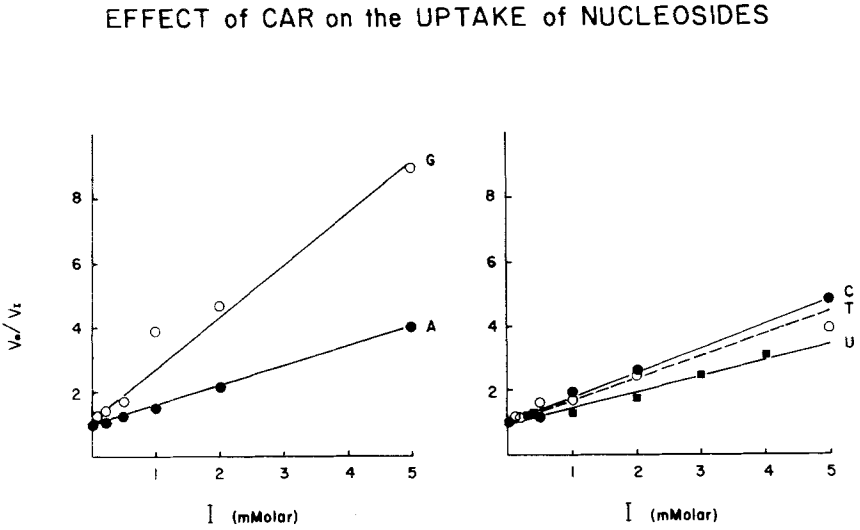

Fig. 9. Inhibition of nucleoside uptake by CAR. Uptake of (^{3}H) nucleosides (1 μM, 2×10^5 cpm/ml) was measured for 5 min in the absence (v_0) or presence (v_i) of increasing concentration of CAR (I) and plotted as in Fig. 8. The ID_{50} values (in μM) were: on A, 1650±410; on B, 650±120; on U, 1920±280; on C, 1400±315; and on T, 1550±365

uptake (v_0/v_I), where the initial uptake v is v_I in the presence and v_0 in the absence of nucleoside I. Among the five nucleosides tested, adenosine and uridine were the most efficient inhibitors of (^{3}H) CAR transport, giving half maximal inhibitory dose (ID_{50}) values of 50 ± 15 and 100 ± 36 μM, respectively. These values are about twofold higher than the K_m values of either adenosine or uridine (Cabantchik and Eilam, *submitted for publication*). Therefore, no definite conclusions could be made regarding the possibility that cytosine-arabinoside and these nucleosides may share a common entry path.

The effect of increasing concentrations of CAR on the uptake of other nucleosides was also studied (Fig. 9). The concentration of S used was $< 1/5$ the K_m value of uptake of the respective nucleoside. CAR did inhibit the uptake of nucleosides, especially the purine ribosides.

Chemical Modification and Inhibition Studies

Nitrobenzylated derivatives of 6-mercaptopurine ribosides are highly potent inhibitors of nucleoside uptake but do not interfere with nucleoside metabolism in broken MCT hamster cell preparations [8, 9]. In this report the most potent member of this class of inhibitors, NBMI, was shown to affect CAR transport in nM concentrations (Fig. 10). The inhibitory effect of NBMI could be further potentiated by chemically modifying cells with the organomercurial *p*-hydroxymercuribenzenesulfonate (*p*MBS), whereas in the same conditions *p*MBS alone stimulated uptake by more than 200%. This indicated that *p*MBS did not increase cell leakiness toward nucleosides, but rendered the cells more susceptible to NMBI. The synergistic effect of *p*MBS and NBMI could also be obtained if cells were first modified with *p*MBS, washed, and then treated with NBMI. Both the individual and the combined effect of these compounds were irreversible, by washing, in the conditions of Fig. 10. Under more strenuous washing conditions, such as multiple washings combined with incubations in PBS, the NBMI effect could be completely reversed, whereas the *p*MBS stimulatory effect could not.

The inhibitory effect of NBMI on nucleoside transport is of a partially competitive nature [9]. Increasing concentrations of NBMI always left a fraction of CAR transport virtually refractive to the inhibitor (Fig. 11). This fraction could be significantly reduced with *p*MBS under conditions where the organomercurial did not inhibit CAR transport, but in fact stimulated it (Fig. 10). The K_i of NBMI on CAR

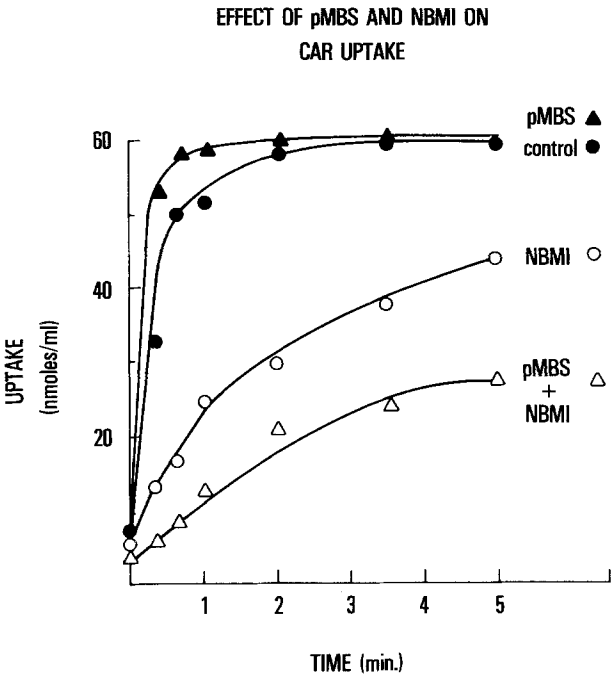

Fig. 10. Effect of inhibitors on CAR transport. Cells (4.2×10^6 per plate, 8.4 µl equivalent volume) were preincubated for 20 min at 22 °C with buffer (control, ●); 50 µM *p*MBS (▲); 20 nM NBMI (○); or 50 µM *p*MBS and 20 µM NBMI (△). The extracellular medium was removed, and the uptake of (^{3}H) CAR (1.4×10^6 cpm/ml, 60 µM) was followed with time

uptake was less than 0.5 nM as measured from the extrapolated line of either the normal or the modified Dixon plot (Fig. 11).[2] It was found, however, that NBMI, at concentrations below 1 nM had a consistent stimulatory effect on CAR uptake (Fig. 11). The level of stimulation relative to control varied from 20 to 50 %, depending on the cell density, time of incubation, and concentration of inhibitor. *p*MBS, in com-

2 At $[S] \ll K_m$, transport in the presence of a competitive inhibitor v_I or in its absence, v_0, are given by:

$$v_0 = \frac{V \cdot [S]}{K_m} \quad \text{and} \quad v_I = \frac{V \cdot [S]}{K_m(1 + [I]/K_i)} \tag{1}$$

and dividing, we obtain

$$\frac{v_0}{v_I} = 1 + \frac{[I]}{K_i}. \tag{2}$$

Thus, a plot of v_0/v_I *vs.* $[I]$ gives a straight line with an intercept equal to $-K_i$.

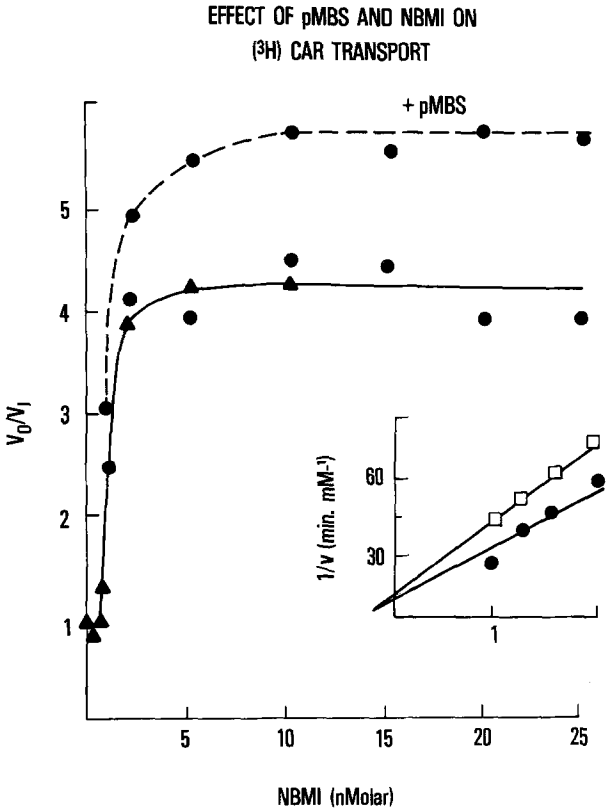

Fig. 11. Dixon plots of NBMI inhibition of CAR transport. Cells were preincubated for 20 min at 22 °C in the presence of increasing concentrations of NBMI without *p*MBS (filled triangles and filled circles represent separate experiments) or in the presence of *p*MBS (50 μM) (open circles). The preincubation media was removed and (^{3}H) CAR (60 μM) uptake was measured as described in Fig. 3. *Inset:* Dixon plot of CAR uptake measured at either 60 μM (●) or 30 μM (□) substrate

bination with low NBMI concentrations, produced only inhibitory effects.

The effect on SH groups was also tested with the relatively more permeable N-ethylmaleimide (NEM). Unlike *p*MBS, NEM inhibits uridine and CAR uptake in hamster cells in culture. The dependence of inhibition of uridine uptake on the concentration and time of reaction of NEM are shown in Fig. 12. Cells were reacted with different concentrations of NEM for 20 min at 20 °C, and washed before uridine uptake was measured. At low concentrations of NEM (up to 10 μM), uptake of uridine was stimulated, but increasing concentrations of inhibitor drastically inhibited the function. A plateau of inhibition (80%)

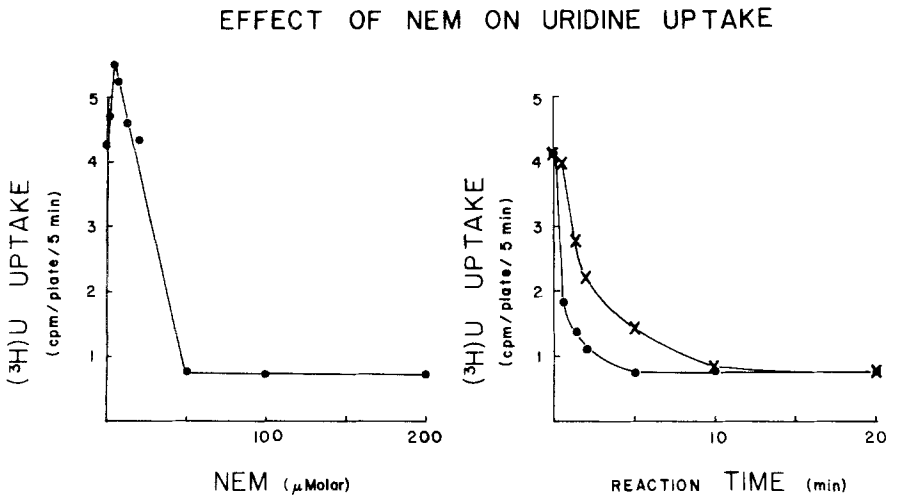

Fig. 12. Profile of inactivation of uridine transport by NEM (N-ethylmaleimide). Cells were exposed to either increasing concentrations of NEM for 20 min at 20 °C (left) or to a constant concentration of NEM [50 μM (×) or 200 μM (●)] for different periods of time (right). Cells were washed 3 times with 5 ml buffer and uptake of (^{3}H) uridine (10 μM) was measured for 5 min at 20 °C

was reached with 50 μM NEM. The reaction times needed to produce half-maximal inhibition with 200 μM and 50 μM NEM at 20 °C were 0.4 min and 1.6 min, respectively. The fall of uptake with time fitted a single exponential decay curve, as expected for inactivation of a single population of SH groups [39].

NEM resembled NBMI in its failure to elicit a full inhibitory effect on uridine uptake. In order to evaluate the NEM effect, uptake of (^{3}H) uridine was followed with time (from 0.5 to 20 min), either concurrent with the NEM reaction (Fig. 13, left) or in cells previously modified with NEM (Fig. 13, right). Uridine uptake was linear up to 20 min at 20 °C. In the presence of maximal inhibitory doses of NEM the inhibitory effect was already apparent at 0.5 min; however, uptake continued at a steady rate even after 20 min. When *p*MBS was added together with NEM, the initial inhibition by NEM was offset by the stimulatory effect of *p*MBS. However, with time, *p*MBS supported inhibition by NEM to levels higher than those attained with NEM alone. This was also shown if cells were first modified with mercurials and uptake of uridine was subsequently measured (Fig. 13, right). Virtually none of the (^{3}H) label associated with cells after 10 min incubation with (^{3}H) uridine, whether in the presence or absence of modifiers, could be identified as (^{3}H)

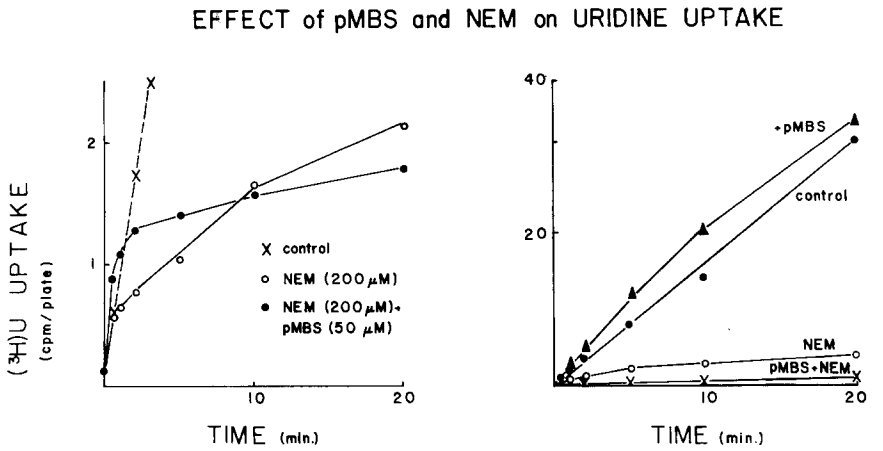

Fig. 13. Effect of SH-reagents on uridine uptake. Cells (1.2×10^6 per plate, 2.4 µl equivalent volume) were incubated with (^{3}H) uridine (10 µM, 1×10^6 cpm/ml) either without inhibitor, with NEM (200 µM), with *p*MBS (50 µM), or with both. *Left:* Uptake of (^{3}H) uridine was measured as a function of time at 20 °C. *Right:* Cells incubated as above for 10 min at 20 °C, washed 3 times with 5 ml buffer and then incubated without inhibitor. Uptake ($\times 10^3$ cpm/plate) is shown as a function of time of the second incubation

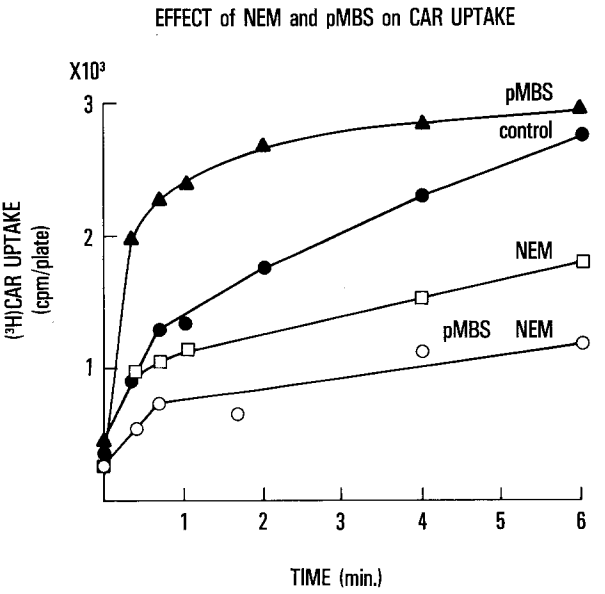

Fig. 14. Effect of SH-reagents on CAR uptake. Cells (2.2×10^6 per plate) were incubated with either *p*BMS *p*MBS, NEM, or *p*MBS and NEM, washed and incubated without inhibitor as in Fig. 12, right. Uptake of (^{3}H) CAR (1 mM, 6.5×10^5 cpm/ml) was measured as a function of time of the second incubation

uridine by thin layer chromatography. Thus, uridine transported into cells was readily metabolized even after substantial modification of cells with maximal transport inhibitory doses of SH blocking agents. It can also be observed that in cells modified with *p*MBS and NEM, the level of (^{3}H) uridine taken up is 1/3 below the internal volume of the cells [(1.7 $\times 10^3$ cpm/2.4 µl cells)$=0.7 \times 10^6$ cpm/ml in cells, as compared with 1 $\times 10^6$ cpm/ml in the external solution] even after 20 min of uptake. This demonstrates that the transport system of (^{3}H) uridine is probably a target of the tested inhibitors. This claim can be further substantiated by studying the effects of *p*MBS and NEM on CAR transport (Fig. 14). Cells modified with these agents display similar behavior toward CAR uptake as toward uridine uptake. Again, *p*MBS significantly stimulated uptake, while NEM partially repressed it. The combined effect of both compounds resulted in more than 95% inhibition.

Discussion

CAR is demonstrated to be a suitable permeant for studying kinetic and chemical properties of nucleoside transport in MCT hamster cells in culture. The main line of evidence is based on the fact that the compound taken up by the cells is not chemically modified for at least a period of 10 min. Thus, unlike the uptake of the metabolizable thymidine and uridine, CAR uptake levels off so that no net accumulation occurs (Figs. 3, 10, 14). The level of CAR attained within the cells relative to the external concentration of substrate yields the same cellular volume as that obtained with another demonstrably nonmetabolizable substrate, 3-O-methyl glucose. On the other hand, in cells capable of fast metabolic conversion of CAR [21], the uptake of profiles of CAR are similar to those obtained with either uridine or thymidine (Fig. 3). Cells lacking the metabolic apparatus for nucleoside modification [22, 27, 28] have invariantly shown profiles of nucleoside uptake similar to those obtained above with CAR. This does not imply that MCT cells are not at all capable of metabolizing CAR, but only that metabolism did not contribute to the results reported here.

CAR uptake (zero-trans influx) at 20 °C is typical of a facilitated diffusion mechanism [36]. It is saturable, and it is inhibited by other nucleosides, by nucleoside analogs, and by some SH reagents. In Yoshida ascites sarcoma cells, CAR is thought to penetrate via the same mechanism used by deoxycytidine and perhaps by other nucleosides [22]. Thus, it is conceivable that nucleoside transport systems may

display a substantial latitude in accepting a variety of nucleosides [1, 12, 27, 28, 35, 37]. However, in the present work (Table 1), the substrate specificity of the nucleoside transport system utilized by CAR remains unresolved. MCT cells may contain manifold nucleoside transport systems with distinct substrate specificities. Although CAR may utilize either one or several of these paths, the fact that a single Michaelis-Menten component (Fig. 5, Table 1) can fully describe the zero-trans properties of CAR influx in the range of concentrations used might argue against multiple paths. However, additional minor transport components of CAR with K_m's either above 10 mM or below 20 μM could easily pass undetected by the techniques of either transport measurements or kinetic analysis used in the present work [4, 10, 35]. Another problem that could affect the kinetic measurements arises from the possible existence of intracellular pools of nucleosides which can exchange with the externally added CAR [26, 28]. In view of the high metabolic rate of the cells, this possibility is remote, but still cannot be ignored [4, 36].

The CAR transport properties have also been characterized in terms of the equilibrium exchange procedure (Fig. 6, Table 1). The advantage of using efflux measurements is that the rate constants, and, consequently, also the influx or efflux parameters, can be accurately measured over a wide range of CAR concentrations without having to measure initial velocities. Also, it circumvents a possible heteroexchange with other nucleosides by having the cells loaded with CAR to equilibrium before isotopic exchange is measured. In the initial analysis of the kinetic data, whether by the linearized or by the nonlinear form of a single Michaelis-Menten component, the resulting V and K_m values of exchange were considerably higher than those of zero-trans (Table 1). Although not uncommon in diffusion-facilitated mechanisms [2, 36], the discrepancy in the V/K_m values indicated an error in the assumption of our analysis. Nonlinear regression analysis (Fig. 7) reveals that in the exchange procedure the lack of saturation at $[S] > 5$ mM could result from the presence of an additional exchange component of either diffusion or high K_m and V [4]. The sum of the two-component system can fit the data as well as a single component system for $[S] < 5$ mM. For higher concentrations, the two component system produces a better fit. The fact that the V/K_m value for the saturable part of the multiple component system is indistinguishable from that obtained in zero-trans conditions (*see* Table 1) also suggests that the two-component system is to be preferred. A similar analytical approach performed on the zero-trans procedure with data up to 1 mM CAR showed that a second transport

component need not be invoked for $[S] < 1$ mM. However, in analogy with the above results, it is conceivable that a second zero-trans component of transport might also be operative at higher CAR concentrations. Unfortunately, the fact that initial velocities of transport could not be accurately obtained at $[S] > 1$ mM precluded us from extending our studies to the relevant concentration levels.

Evidence for the existence of two saturable components of CAR transport has also been recently demonstrated in Yoshida ascites sarcoma cells [22].

Modulation of Nucleoside Transport Activity with Chemical Probes

The addition of nM amounts of NBMI to MCT cells results in inhibition of CAR transport and of nucleoside uptake into cells (Figs. 10, 11), [8, 9]. Based on the assumption that these nucleosides share common transport systems which are sensitive to NBMI and that NBMI does not interfere directly with their metabolic conversion [9], we concluded that the inhibitor acted directly on the transport component of nucleoside uptake. The profile of NBMI inhibition previously found for uridine uptake [8, 9] was reproduced for CAR transport (Fig. 11). The inhibitions were reversible and were apparently of a partially competitive nature [39, 40], displaying K_i values of less than 0.5 nM. The effects were competitive inasmuch as the percent inhibition relative to control decreased with increasing concentration of substrate at constant concentration of inhibitor and, as a consequence, the appropriate K_m increased. They were of partial nature since increasing concentrations of inhibitor at constant substrate concentration led to a finite inhibitory level which was substantially lower than 1.0 (Fig. 11).

These features were previously explained by assuming NBMI binding to a carrier I at sites different from the substrate binding sites (i.e., allosteric sites) [20] and inducing a conformational change ($I_A \xleftrightarrow{\text{NBMI}} I_B$) [8]. This change is manifested in a decreased affinity of I for the substrate and an increased susceptibility to *p*MBS (Fig. 15, model 1). Alternatively the NBMI-refractive fraction of nucleoside transport might represent an additional nucleoside entry path *II* which is insensitive to NBMI, but can be inhibited by *p*MBS (Fig. 15 is model 2). The difference between the two models resides primarily in the "nature" of the competitive inhibition by NBMI: in model *2* it is exerted via binding to

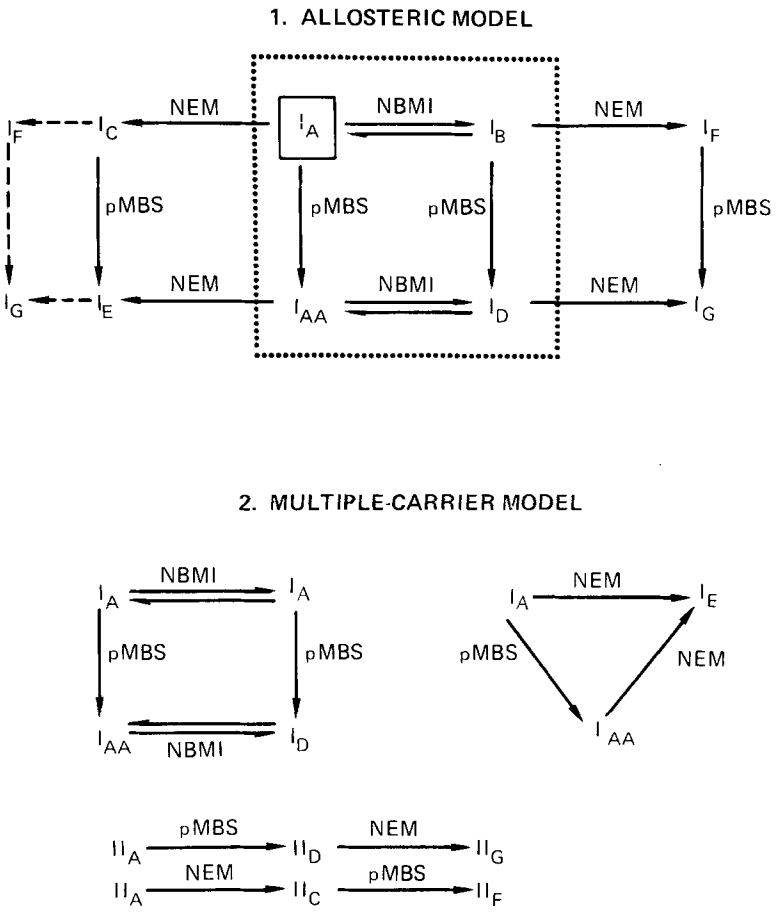

Fig. 15. Hypothetical models for nucleoside transport systems. (*1*): The *allosteric model* assumes a single carrier I which can adopt distinct conformations $A-G$ upon modification by various probes. I_A represents the unmodified carrier which can be either stimulated by *p*MBS, inhibited in a partially-competitive fashion by NBMI or noncompetitively by NEM. The relative transport activity of the system in the various states is in the following order: $I_{AA}>I_A>I_B>I_C>I_D>I_E>I_F>I_G$. The reaction scheme inside the square that is demarked by dotted lines is based on data presented in our previous works [8, 9]. (*2*): The multiple carrier model assumes two carriers, I_A and II_A, operating in parallel. For a given nucleoside, I_A represents its predominant carrier which can be inhibited by either NBMI (fully competitive fashion) or NEM (fully noncompetitive fashion) and can also be stimulated by *p*MBS. II represents a carrier which is insensitive to NBMI but is inhibited by SH reagents in either a partially or fully noncompetitive fashion

substrate sites and it can be "complete", whereas in model *1* it is exerted on allosteric sites and it is only of a partial nature.

Although a kinetic analysis presented elsewhere [9] and the fact that *p*MBS alone did not produce inhibition tended to make *1* the model of preference, the actual need to imply allosteric sites for structurally related analogs of the substrate can be questioned. We observed that the organomercurial alone highly stimulates transport of either CAR or uridine (Figs. 10, 13, 14). It is therefore possible that *p*MBS actually inhibited component *II* but the effect was overshadowed by the marked stimulation of the predominant component *I*. In this case NBMI alone or NBMI in combination with *p*MBS will inhibit component *I*, while *p*MBS alone will inhibit only component *II* (Fig. 15). The experiments with the irreversible binding reagent NEM may support the latter view. Unlike *p*MBS, NEM inhibits nucleoside transport very efficiently, but like NBMI, it leaves a residual transport activity refractive to increasing concentrations of reagent. Again, this activity can be abolished by *p*MBS added before, after, or during NEM reaction (Figs. 13, 14). Although these results are compatible with either model (Fig. 15), it will be difficult to envisage two agents as dissimilar as NBMI and NEM either acting by analogous mechanisms or producing similar effects, as required in Model *1*. Model *2*, provides a simpler explanation by invoking the involvement of two transport systems, one susceptible to NBMI and/or NEM inhibition and another susceptible to inhibition by *p*MBS (Fig. 15). This model is also compatible with the results of CAR exchange which can be interpreted in terms of two transport systems acting in parallel, one displaying low K_m properties and the other displaying either a high K_m or simple diffusion properties (components I_A and II_A, respectively, in Fig. 15, Model *2*). The observation that CAR transport can be fully inhibited by a combination of nucleoside analogs and chemical modifiers indicates that component *II* might constitute a specific transport system with saturable properties.

Nucleoside transport systems differ considerably in their response to various SH blocking reagents, particularly organomercurials. When separately applied, *p*MBS and NEM have opposite effects – the former stimulates, whereas the latter inhibits transport. However, when applied together or in series (in either order), NEM reverses or abolishes the stimulation and elicits an inhibition of its own which is higher than that produced with *p*MBS absent. Stimulatory and synergistic effects have also been obtained with the nonpenetrating mercurial *p*MB-dextran and NEM, but none of these effects have been observed with either iodoacet-

amide (IAA), iodoacetic acid (IA) or bis-dithionitrobenzoic acid (DTNB) (*unpublished observations*). Thus, results with the lipophylic NEM and with the hydrophylic mercurials suggest the involvement of heterogeneous populations of SH groups in transport of nucleosides. The groups related to stimulation are likely to be at the exterior of the membrane since they are accessible to either *p*MBS or *p*MB-dextran [30]. Those related to inhibition are internally located in the membrane, easily in the reach of reagents as NEM, but inaccessible to organomercurials. Although NEM is also likely to react with external SH groups, the putative stimulatory effect was not observed except at very low concentrations of reagent (Fig. 12), where NEM is expected to react preferentially with superficial sites.

It is conceivable that the topological differences of these functional-related groups are a result of their being associated with different membrane proteins, some of which are directly involved in transport. It is also conceivable that stimulation of a transport system resulted from neutralization of SH-containing entities which inhibited the function. However, results obtained in this work (Figs. 10, 11, 12, 14) would indicate that *p*MBS supports or potentiates subsequent inhibition by either NEM or NBMI, probably by modifying the conformation of the transport systems to "states" more susceptible to the aforementioned probes (Fig. 15). These conclusions stem from the fact that the combined effects of the various agents could not be explained solely on the basis of additive effects.

Stimulation of transport processes by SH reagents has previously been observed in other systems [6, 30, 34], although not with nucleosides [7, 13, 28]. We have observed both stimulatory and potentiating effects of *p*MBS on nucleoside transport in a variety of normal and transformed hamster and mouse cell lines and we are exploring their function in the modulation of transport processes by physiological factors. Stimulatory effects of various components on glucose transport in thymocytes have been recently described [40].

This work was supported by a grant from the USA-Israel Binational Science Foundation (BSF), Jerusalem to Z.I.C. and by the NCI contract No. NO1 CP 43307 to W.D. Stein. Z.I.C. was a Lady Davis Fellow of the Hebrew University.

We gratefully acknowledge Mrs. L.T. Hirz for typing this manuscript.

References

1. Berlin, R.D., Oliver, J.M. 1973. Membrane transport of purine and pyrimidine bases and nucleosides in animal cells. *Int. Rev. Cyt.* **212**:287

2. Cabantchik, Z.I., Ginsburg, H. 1977. Transport of uridine in human red blood cells. Demonstration of a simple carrier-mediated mechanism. *J. Gen. Physiol.* **69**:75
3. Cass, C.E., Paterson, A.R.P. 1975. Inhibition by nitrobenzylthioinosine of uptake of adenosine, 2′-deoxyadenosine and 6-β-D-arabinofuranosyladenine by human and mouse erythrocytes. *Biochem. Pharmacol.* **24**:1989
4. Christensen, H.N. 1975. Biological Transport. pp. 136–142. W.A. Benjamin, London
5. Cunningham, D.D., Pardee, A.B. 1969. Transport changes rapidly initiated by serum addition to "contact inhibited" 3T3 cells. *Proc. Nat. Acad. Sci. USA* **64**:1049
6. Czech, M.P. 1976. Differential effects of SH reagents on activation and deactivation of the fat cell hexose transport system. *J. Biol. Chem.* **251**:1164
7. Dosckocil, J. 1976. The role of thiol groups in nucleoside transport. *Mol. Cell. Biochem.* **10**:137
8. Eilam, E., Cabantchik, Z.I. 1976. The mechanism of interaction between high affinity probes and the uridine transport system of mammalian cells. *J. Cell. Physiol.* **89**:381
9. Eilam, E., Cabantchik, Z.I. 1977. Nucleoside transport in mammalian cell membranes. II. A specific inhibitory mechanism of high affinity probes. *J. Cell. Physiol.* **92**:185
10. Goldman, I.D. 1976. Uptake of drugs and resistance. *Adv. Exp. Med. Biol.* **69**:299
11. Hakala, M.T. 1976. Enzyme changes in resistant tissues. *Adv. Exp. Med. Biol.* **69**:263
12. Hakala, M.T., Kenny, L.N. 1972. Common mechanism for the passage of purine and pyrimidine nucleosides through the plasma membrane of sarcoma 180 cells (C-180). *Fed. Proc.* **31**:457
13. Hare, J.D. 1975. Distinctive alterations of nucleoside, sugar and amino acid uptake by sulfhydryl reagents in cultured mouse cells. *Arch. Biochem. Biophys.* **170**:347
14. Hochstadt, J. 1974. The role of the membrane in the utilization of nucleic acid precursors. *CRC Crit. Rev. Biochem.* **2**:259
15. Hochstadt, J., Quinlan, D.C., Rader, R.L., Li, C.C., Dowd, D. 1976. Use of isolated membrane vesicles in transport studies. *In:* Methods in Membrane Biology. Vol. 5, ch. 3. E. Korn, editor. Plenum Press, New York
16. Holley, R.W. 1972. A unifying hypothesis concerning the nature of malignant growth. *Proc. Nat. Acad. Sci. USA* **69**:2840
17. Huberman, E., Yamasaki, H., Sachs, L. 1974. Genetic control of the regulation of cell susceptibility to carcinogenic polycyclic hydrocarbons by cyclic AMP. *Int. J. Cancer* **14**:789
18. Kessel, D., Hall, T.C., Rosenthal, D. 1969. Uptake and phosphorylation of cytosine arabinoside by normal and leukemic human blood cells in vitro. *Cancer Res.* **29**:459
19. Kessel, D., Shurin, S.B. 1968. Transport of two nonmetabolized nucleosides, deoxycytidine and cytosine-arabinoside in a sub-line of the L1210 murine leukemia. *Biochim. Biophys. Acta* **163**:179
20. Monod, J., Wyman, J.N., Changeux, J.P. 1965. On the nature of allosteric transitions: A plausible model. *J. Mol. Biol.* **12**:88
21. Montgomery, J.A., Johnston, T.P., Gallagher, A., Stringfellow, C.R., Schabel, F.M. 1961. A comparative study of the anticancer activity of some S-substituted derivatives of 6-mercaptopurine and their ribosides. *J. Med. Pharm. Chem.* **3**:265
22. Mulder, J.H., Harrap, K.R. 1975. Cytosine arabinoside uptake by tumor cells in vitro. *Eur. J. Cancer* **11**:373
23. Oliver, J.M., Paterson, A.R.P. 1970. Nucleoside transport: 1. Mediated process in human erythrocytes. *Can. J. Biochem.* **219**:262
24. Pardee, A.B., Palmer, L.M. 1973. Regulation of transport systems. A means of controlling metabolic states. *Proc. Soc. Exp. Biol.* **27**:133
25. Paul, B., Chen, F.M., Paterson, A.R.P. 1975. Inhibition of nucleoside transport. A structure-activity study using human erythrocytes. *J. Med. Chem.* **18**:968

26. Plagemann, P.G.W. 1971. Nucleoside transport by Novikoff rat hepatoma cells growing in suspension culture. Specificity and mechanism of transport reactions and relationship to nucleoside incorporation into nucleic acids. *Biochim. Biophys. Acta* **233**:688
27. Plagemann, P.G.W., Marz, R., Erbe, J. 1976. Transport and counter-transport of thymidine in ATP depleted and thymidine-kinase deficient Novikoff rat hepatoma and mouse cells: Evidence for a high K_m facilitated diffusion system with wide nucleoside specificity. *J. Cell. Physiol.* **89**:1
28. Plagemann, P.G.W., Richey, D.P. 1974. Transport of nucleosides, nucleic acid bases, choline and glucose in animal cells in culture. *Biochim. Biophys. Acta* **377**:263
29. Quinlan, D.C., Hochstadt, J. 1976. Group translocation of the ribose moiety of inosine by vesicles of plasma membrane from 3T3 cells transformed by Simian Virus 40. *J. Biol. Chem.* **251**:344
30. Rothstein, A. 1970. Sulfhydryl groups in membrane structure and function. *In:* Current Topics in Membranes and Transport. F. Bronner, A. Kleinzeller, editors. Vol. 1, pp. 135–176. Academic Press, New York
31. Schrecker, A.W. 1970. Metabolism of 1-β-D-arabinofuranocylcytosine in leukemia 1210: Nucleoside and nucleotide kinase in cell free extracts. *Cancer Res.* **30**:632
32. Schrecker, A.W., Urshel, M.J. 1968. Metabolism of 1-β-D-arabinofuranocylcytosine in leukemia 1210: Studies with intact cells. *Cancer Res.* **28**:793
33. Simon, B., Zimmerschied, G., Kinne-Saffran, E.M., Kinne, R. 1973. Properties of a synthetic plasma membrane marker: Fluorescent-mercury-dextran. *J. Membrane Biol.* **14**:85
34. Spooner, P.M., Edelman, I.S. 1976. Stimulation of Na^+ transport across the toad urinary bladder by *p*-chloromurcuribenzene sulfonate. *Biochim. Biophys. Acta* **455**:272
35. Steck, T.L., Nakata, Y., Bader, J.P. 1969. The uptake of nucleosides by cells in culture. I. Inhibition by heterologous nucleosides. *Biochim. Biophys. Acta* **190**:237
36. Stein, W.D. 1967. The Movement of Molecules Across Cell Membranes. Academic Press, New York
37. Taube, R.A., Berlin, R.D. 1972. Membrane transport of nucleosides in rabbit polymorphonuclear leukocytes. *Biochim. Biophys. Acta* **255**:6
38. Vignais, P.M., Chabert, J., Vignais, P.R. 1976. The use of sulfhydryl reagents to identify proteins undergoing conformational changes in mitochondrial membrane. *Biochim. Biophys. Res. Commun.* **72**:307
39. Webb, J.L. 1963. Enzyme and metabolic inhibitors. Academic Press, New York
40. Whitsell, R.R., Hoffman, L.H., Regen, D.M. 1977. Dynamic aspects of glucose transport modulations in thymocytes. *J. Biol. Chem.* **252**:3533
41. Zeffren, E., Hall, P.L. 1973. The study of enzyme mechanism. John Wiley & Sons, New York